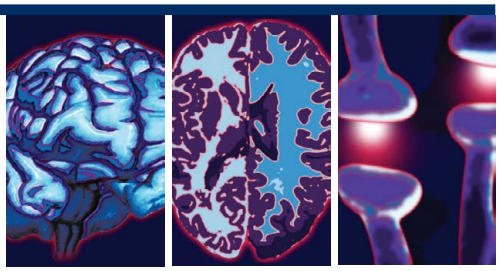

A Feasibility Research on Restoration of Demyelination in Trigeminal Nerve with Transnasal Administration of BDNF/NGF Loading on PEG-PLA Nanoparticles

Lei Xia, Jun Zhong†, Ming-Xing Liu, Ning-Ning Dou, Bin Li

Abstract

Background

Trigeminal neuralgia (TN) is caused by the vascular compression of the Vth cranial nerve root, where the pathology of demyelination has been observed. Although microvascular decompression surgery has become the most reasonable technique for the treatment, this sort of operation is with risk and invasive. Accordingly, we attempt to find a noninvasive approach to treat TN.

Methods

Sprague Dawley (SD) rats were used for the experimental series. The brain-derived neurotrophic factor (BDNF) and nerve growth factor (NGF) were used to restore the demyelization of trigeminal nerve, which were loading on poly (ethylene glycol)-poly (lactic acid) (PEG-PLA) nanoparticles. After nasal administration, then the nanoparticles were tracked with a vivo imaging system. The TN model was established by chronic constriction injury of the infraorbital nerve. Some rats that only underwent exposure of infraorbital nerve without ligation served as *group sham*. Those successful TN rats were randomly allocated to *group TN+BDNF*, *group TN+NGF* and *group TN*. After administration of BDNF-NPs and NGF-NPs as well as normal saline in different groups, then the mechanical allodynia was tested. Finally, all the animals were killed and the trigeminal nerve specimen was ready for electron microscopy, Western-Blotting, RT-PCR, CCK8 assay and immunostainingof S-100.

Results

The synthesized BDNF-NPs/NGF-NPs has a mean diameter and encapsulation efficiency of 129.8 nm/128.6 mm and 83.9%/79.5% with a release rate of 87.6%/85.3% (7 days later), respectively. The fluorescence signals of the nanoparticles appeared in the trigeminal nerve as early as 5 min, and became stronger at 30 min. Three weeks after the nasal administration, the mechanical allodynia didn't change apparently in *group Sham* and *group TN*, while it significantly increased in *group TN+BDNF* and *group TN+NGF*. The microscopy exhibited that intact myelins with homogeneous density of axon in *group TN+BDNF* and g*roup TN+NGF* as well as in *group sham*, while the axons and myelin sheaths were absent in *group TN*. The results of Western-Blotting and RT-PCR indicated that the level of $Na_v1.8$ and Bax were significantly increased in *group TN* compared with other groups ($p<0.05$). But the level of Bcl-2 and NF-κB were significantly increased in *group TN+BDNF and TN+NGF* compared with *group TN* ($p<0.05$).

Department of Neurosurgery, XinHua Hospital (The Cranial Nerve Disease Center of Shanghai), Shanghai JiaoTong University School of Medicine, China

†Author for correspondence: Jun Zhong, Department of Neurosurgery, XinHua Hospital (The Cranial Nerve Disease Center of Shanghai), Shanghai JiaoTong University School of Medicine, Shanghai 200092, 1665 Kong Jiang Rd, Shanghai 200092, China, Tel: 021-25078021; Fax: 021-25078025; email: ZhongJun@XinHuaMed.com.cn

The CCK-8 and Immunostaining of S-100 experiments indicated that the BDNF-NPs or NGF-NPs could promote the expression of Schwann cells ($p<0.05$).

Conclusions

The study demonstrated that BDNF/NGF loading on nanoparticles may transmit along with the trigeminal nerve via nasal administration and facilitate the restoration of myelin sheath. It could be a sort of noninvasive remedy for trigeminal neuralgia.

Keywords

Trigeminal neuralgia; PEG-PLA nanoparticles; Nerve growth factor; Brain-derived neurotrophic factor; Intranasal administration; Demyelination

Introduction

Trigeminal neuralgia (TN) is one of the most painful conditions in human clinical practices, which is defined as unilateral disorder characterized by brief electric shock-like pains limited to the distribution of one or more divisions of the trigeminal nerve [1-5]. It is etiologically caused by vascular compression of the trigeminal root, no matter directly or indirectly pushed by neoplasms or adhesions in the cerebellopontine angle [6-8]. It was speculated that an ephaptic transmission or ectopic impulse occurred at the micro-injury site of the trigeminal nerve fibers compressed by a vessel [9]. Whatever, it has been widely accepted that the at the vascular compressed site is the precondition of TN generation[10]. Although the microvascular decompression surgery has been thought to be the most reasonable technique for treatment of TN, this sort of operation is still with risk because of those delicate structures in the operative field [11-13]. Sometimes, a life-threatening complication may occur[12]. Accordingly, it would be better if we can find a new approach to treat TN noninvasively.

As the BDNF or NGF have been proved to be capable to promote the regeneration of myelin sheaths in axons, it might be possible to cure TN via restoration of the demyelination [14,15]. Nevertheless, the application of BDNF or NGF is restricted due to its poor permeability through the blood-brain barrier (BBB). Recently, it has been demonstrated that intranasal administration of vasoactive intestinal peptide (VIP) conjugated with PEG-PLA nanoparticles was a promising method for protecting peptides from peptidase degradation and enhancing transport of peptides to the CNS [16]. With this technology, the bioavailability of intact VIP in mice brain was significantly increased by 5.6-7.7 folds and 1.58-1.82 folds, compared with intranasal solution and unmodified nanoparticles, respectively [16]. The trigeminal nerve enters the brainstem at the pons and some of its nerve endings terminate beneath the nasal epithelial surface, which provides possible entrance for intranasally administrated nanoparticles into the brain. The diameter of trigeminal nerve endings is about 0.2-1.5 μm while nanoparticles has a particle size smaller than 0.2 μm, so nanoparticles might be transported along trigeminal nerve via intracellular mechanisms (propelled by axonal flow) [17]. Although there are considerable researchs indicated that intranasal delivery of BDNF or NGFcould be a method to repair the axon and myelination, no studies have investigated BDNF-NPs / NGF-NPs whether could be a promising delivery system to treat the TN in SD rats.

Materials and Methods

■ Animals

Adult Sprague-Dawley rats (Shanghai, China) of either gender (weighed between 250-350 g) were used in this study. The animals were maintained in solid-bottom cages in a colony room with a humidity of 40-60% and the temperature-controlled room (23 ± 1°C) with a 12/12 hour light-dark cycle. Water and food were available. All experimental procedures were approved by the Animal Care and Use Committee for Research and Education of the Shanghai JiaoTong University School of Medicine. All efforts were made to minimize the animal suffering and to reduce the number of animals used.

■ Preparation of PEG-PLA nanoparticles loaded with BDNF or NGF

PEG-PLA nanoparticles (NP) were prepared by the emulsion/solvent evaporation method. Briefly, MePEG-PLA (22.5 mg) and Male-PEG-PLA (2.5 mg) were gifted from Sichuan university of electronic science and technology and were dissolved in 1 ml of dichloromethane and added

into 2 ml of 1% sodium cholate, followed by emulsion at 280 w for 1 min. The o/w emulsion was then dispersed in 20 ml of 0.5% sodium cholate and magnetically stirred for 5 min. After dichloromethane evaporation, the nanoparticles were concentrated by centrifugation (14000 r/min ×45 min, 4℃).

This part was prepared by the double emulsion/solvent evaporation method. PEG-PLA (25mg) were dissolved in 1 ml of dichloromethane solution, and then join in the inner phase (50 μL) (BSA: 4 mg/ml; BDNF or NGF: 400 μg/ml). Five minutes later, dichloromethane was evaporated at low pressure at 30°C using Büchi rotavapor R-200 (Büchi, Germany). Then the nanoparticles were collected by centrifugation at 14000 r/min for 45 min using TJ-25 centrifuge (Beckman Counter, USA.) equipped with A-14 rotor and washed with water for three times to removed the BDNF or NGF unentrapped or adsorbed to the exterior of the nanoparticles. Finally, the nanoparticles loaded with BDNF or NGF (R&D Systems) were synthesized. The concentration of the BDNF or NGF was 25 mg/ml in the nanoparticles. These nanoparticles (BDNF-NPsor NGF-NPs) were ready for the animal and cell experiments. The morphological examination of nanoparticles was performed by transmission electron microscopy (TEM) (H-600, Hitachi, Japan) following negative staining with sodium phosphotungstate solution.

■ Tracking of BDNF-NPs or NGF-NPs following transnasal administration

The animals were anesthetized with pentobarbital (40mg/kg) (Sigma, USA) and given 0.5mg of 1,1′-dioctadecyl-3,3,3′,3′-tetramethy l indotricarbocyanine Iodide (DiR) (Biotium, USA) loaded with BDNF-NPs or NGF-NPs via the right nostril. 5min, 30min, 2h, 6h, 12h and 24h after administration, the animals were executed respectively. The brainstem was separated and microdissected with a scalpel carefully. The trigeminal nerve was isolated from bone tissue of skull base and dissected from the root of trigeminal nerve to the anterior lacerated foramen and the foramen ovale. The olfactory bulb was also isolated from bone tissue of skull base. These samples were carefully isolated and visualized by Cri in vivo imaging system (MA, USA). Measurements were made on three rats each time point. Then the fluorescence signals were analysised semi-quantitatively.

■ Surgical procedures for preparation of trigeminal neuralgia model

The animals were anesthetized with pentobarbital (40 mg/kg). The surgery was performed on the right sides of the experiment animals under direct visual control using a Zeiss surgical microscope (Carl Zeiss, Inc., Jena, Germany). The rats were taped to a sterilized cork board, and the skin above the eye was shaved. Lubricating ophthalmic ointment was applied to the eyes to prevent drying damage. An anterior-posterior skin incision approximately 7 mm long is made 2 mm above the left eye, following the curve of the frontal bone. The fascia and muscle were then gently teased laterally from the bone to retract the contents of the orbit laterally. Once the orbital contents were gently deflected, the right infraorbital nerve (ION) could be seen lying on the infraorbital groove of the maxillary bone within the orbit. The superior surface of the ION was then separated. Once visible, at least 5 mm long of the ION must be gently freed from the surrounding connective tissue with fine jeweler's forceps using the spreading technique in order to place the 2 ligatures. Approximately 0.5 cm of the ION was freed of adhering tissue, and two 5.0 polyglycolic acid ligatures were tied loosely around it. Slide the knot further to constrict the ION so that the diameter of the nerve is reduced by a just noticeable amount. The incision above the eye was sutured at two points using 4.0 silk and the rat allowed to recover. For the sham-operation animals, they were subjected to the identical anesthetic and exposure of the infraorbital nerve was just exposed without ligature. Two weeks after the surgery, the animals underwent allodynia test and those with obvious low pain threshold were regarded as a success TN animal model.

■ Mechanical allodynia

The mechanical testing procedure was modified from previous described methods [18]. The animals were placed in a small metal cage (30×25×20 cm) to habituate for 30 minutes before threshold testing. A logarithmic series (0.41, 0.70, 1.20, 2.00, 3.63, 5.50, 8.50, and 15.10g) of calibrated Semmes-Weinstein monofilaments (von Frey hairs; Stoelting, Kiel, WI, USA) were applied to test mechanical stimulation in the vibrissa pad of the animals to determine the stimulus intensity threshold stiffness to elicit a brisk head with drawal response. Stimulations were administered when the rat was in a sniffing/no locomotion position.

When the rat stopped exploratory behavior and ceased major grooming, the stimuli were applied within the ION territory. A von Frey hair was held for approximately 5 seconds and presented at intervals of several seconds based on the elimination of the behavioral responses to previous stimuli. A clear withdrawal response was recognized as follows: (1) rat avoids further contact with the monofilament, (2) rat turns head rapidly away scratching the stimulated area, (3) or rat actively attacks the stimulating object. The mechanical threshold of withdrawal response was measured according to the up-down method and thus the 50% threshold was computed using the formula described by Dixon [18].

■ Animal grouping

The animals were randomly allocated to four groups. *Group Sham*, those only underwent sham operation and received nothing. *Group TN*, those TN model rats received only normal saline. *Group TN+BDNF*, those TN model rats received BDNF-NPs. *Group TN+NGF*, those TN rats received NGF-NPs.

■ Administration

After anesthesia, the animals were placed supine with the head upright. Five drops (5 μl/drop) of normal saline, BDNF-NPs or NGF-NPs were administered through the right nostril in 3-5 minutes. The protocol was repeated for 7 days. After that, the mechanical allodynia was tested at day 1, 3, 7, 14 and 21. Finally, these animals were killed with cervical dislocation and 5-mm long trigeminal nerve samples around the ligated point were obtained for the next experiments.

■ Electron microscopy

The trigeminal nerve specimen was phosphate-buffered and fixed in 2.5% glutaraldehyde solution (pH 7.4) for 2 hours. After being washed 3 times with buffered solution, it was exposed to 1% osmium tetroxide for 1 hour as post-fixation. Staining was achieved with 1% aqueous uranyl acetate, followed by dehydration with an ethanol gradient and treatment with propylene oxide. Finally, the specimen were infiltrated and embedded in pure epoxy.

■ Western-blotting

The trigeminal nerve specimens were homogenized in a RIPA lysis buffer containing protease inhibitions (Applygen Technologies Inc., China). Protein concentrations of the lysate were determined using a BCA Protein Assay Kit (USA). The specimen were heated for 10 min at 95°C with SDS-PAGE sample buffer, and equal amounts of protein were then separated by 10% separation gels. The resolved proteins were subsequently transferred to nitrocellulose membranes (Bio-Rad, Hercules, CA, USA) followed by the incubation with 5% nonfat milk (Bio-rad, CA, USA) in PBS with 0.05% Tween 20 (PBST) for at least 30 min at room temperature. Then, the membranes were incubated with primary antibodies at 4°C overnight. The membranes were visualized with enhanced chemiluminescencce solution (Alpha Innotech Corp.), and the signals were captured with Fluor Chem FC2 (Alpha Innotech Corp.). The density of specific bands was measured with a computer-assisted imaging analysis system (Bio-Rad, CA, USA) and normalized to β-tubulin intensity.

■ RNA and qRT-PCR analysis

The real-time quantitative polymerase chain reaction (qRT-PCR) was used to analysis the gene expression of Nav1.8, NF-κB, Bax and Bcl-2 in these four groups. RSCs were seeded on PLGA scaffolds in 6-well plates and cultured alone or with NECL 1 (concentrations of 25, 50, and 100ng/ml). Seven days later, RNA was extracted with a total isolation RNA kit (Invitrogen, USA) according to the instruction of manufactures. The qRT-PCR reactions were performed using a quantitative PCR detection system with a Fast Start University SYBR Green Master under the condition of 10min at 95°C, 15 s at 95°C and 1 min at 60°C. The mRNAs of these proteins and GAPDH (internal control) were listed below **(Table 1)**. Relative gene expression levels were calculated using the 2-ΔΔCt method using glyceraldehyde-3-phosphate dehydrogenase (GAPDH) gene expression.

■ Cell culture

The fresh trigeminal nerve specimens were cut into pieces before enzymatic digestion was started with 0.2% collagenase A (Roche Applied Science, Indianapolis, IN). Every 30 min, dissociated cells were harvested by centrifugation at 200 g for 5 min, and the collagenase solution was reused for further digestion of trigeminal nerve. The pellet was resuspended in culture medium (Neurobasal Medium supplemented with 2% B-27 and 2 mM L-glutamine; Life Technologies, Grand Island, NY), and the cells were plated on polylysine and laminin-coated 24-well tissue culture plates (BD Bioscience, Franklin Lakes, NJ). 6 hours later, these cells were ready for observation by electron microscopy (TEM) (H-600, Hitachi, Japan).

Table 1: Primer sequences used in qRT-PCR experiments.

Gene	Primer sequence (5' to 3')	Amplified product	
		Size (bps)	Product GC (%)
$Na_v1.8$	F 5' GGCATTCCTCTCACTGTTC 3' R 5' CTGGCTCTGCTCTTCATAC 3'	184	53
NF-kB	F 5' AGACCTGGAGCAAGCCATTAG 3' R 5' CGGACCGCATTCAAGTCATAG 3'	102	54
Bax	F 5' GGACGCATCCACCAAGAAG 3' R 5' CTGCCACACGGAAGAAGAC 3'	134	55
bcl-2	F 5' GGGATGCCTTTGTGGAAC 3' R 5' GTCTGCTGACCTCACTTG 3'	148	58
GAPDH	F 5' GTCGGTGTGAACGGATTTG 3' R 5' TCCCATTCTCAGCCTTGAC 3'	181	51

NF-kB, Nuclear factor kB; GAPDH, glyceraldehyde-3-phosphate dehydrogenase; F: forward primer; R: reverse primer

■ CCK8 assay

Cell growth and viability were using cell proliferation reagent WST-8 and cultured in a 96-well plate. After 12h, the cell growth and viability were calculated. At the harvest time, 10 μl of CCK8 was added into each well and after one hour's incubation cell viability was determined by measuring the absorbance of the converted dye at 490 nm. The experiments were triplicate.

■ Immunostaining

The cells cultured on chamber slides were fixed in 4% paraformaldehyde at 4°C for 20 min. The cells were then incubated overnight at 4°C with primary antibodies against S-100 (rabbit polyclonal; 1:200; Santa Cruz, USA). The following day, the slides were incubated for 2 h with the secondary antibody (goat antirabbit; 1:100; Sigma, USA). The slides were examined under a microscope (Olympus SZ51) and the numbers of immuno-positive cells were counted in a minimum total of 100 cells per experiment.

■ Statistical analysis

Statistical analyses were performed using GraphPad 6 software (GraphPad 6 software Inc., San Diego, CA, USA). The data were expressed as Mean ± SEM and one-way analysis of variance (ANOVA). All the data were collected at least in triplicate or each group. The differences were considered significant when $p<0.05$.

Results

■ The nanoparticles

The synthesized BDNF-NPs/NGF-NPs has a mean diameter and encapsulation efficiency of 129.8 nm/128.6 mm and 83.9%/79.5% (**Figure 1a/b**), respectively. In vitro, at day 1 and day 7, the BDNF-NPs/NGF-NPs release rate was 35.2%/36.5% and 87.6%/85.3%, respectively (**Figure 2**).

Distribution of nanoparticles following intranasal administration of BDNF-NPs or NGF-NPs was measured and the levels of radioactivity in brainstem, olfactory bulb and trigeminal nerve were shown in **Table 2**. Nasal absorption of the nanoparticles into the systemic circulation was rapid. The main fluorescence signals of nanoparticles appeared in the brain stem, olfactory bulb and trigeminal nerve as early as 5 min, and became stronger at 30 min. The trigeminal nerve showed significant higher radioactivity than the brainstem and the olfactory bulb. Two hours later, the radioactivity in all the samples were faded (**Figure 3**).

■ Mechanical allodynia

Three weeks after the administration, the mechanical allodynia didn't change apparently in *Group Sham* and *Group TN*, while it significantly increased in *Group TN+BDNF* and *Group TN+NGF*. Nevertheless, it occurred a transient decrease in *group TN + NGF* at day 7 (**Figure 4**).

■ Electron microscopy

Twenty-one days after the administrations, the microscopy exhibited that intact myelins with homogeneous density of axon in *Group Sham*, while severe demyelination in *Group TN*. However, *Group TN+BDNF* and Group TN+NGF didn't exhibited much different compared to the *Group Sham* (**Figure 5**).

■ Western blot assay

In order to study the anti-apoptosis effect of BDNF or NGF, we examined the expression of Nav1.8, NF-κB, Bcl-2 and Bax protein of

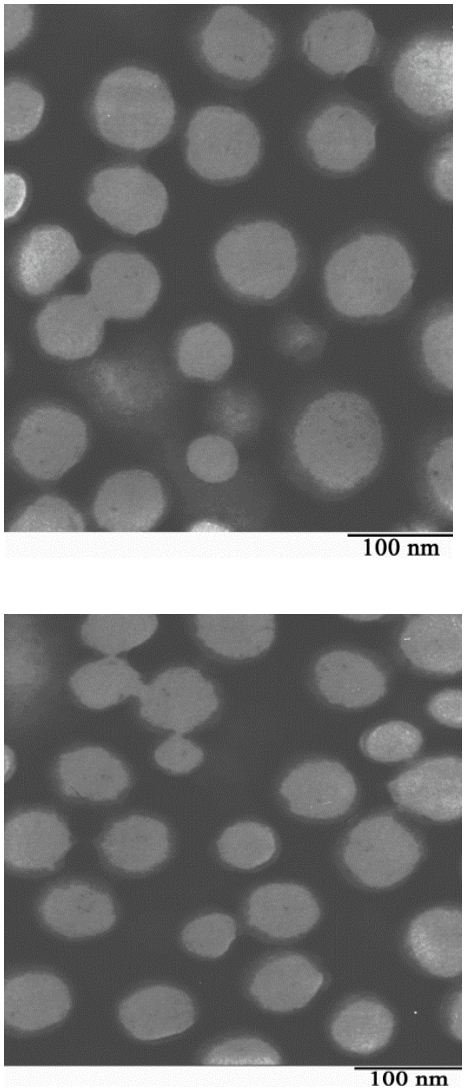

Figure 1: Transmission electron micrograph delineating BDNF loading on PEG-PLA nanoparticles (a) Transmission electron micrograph delineating NGF loading on PEG-PLA nanoparticles (b) *Scale bar = 100* nm.

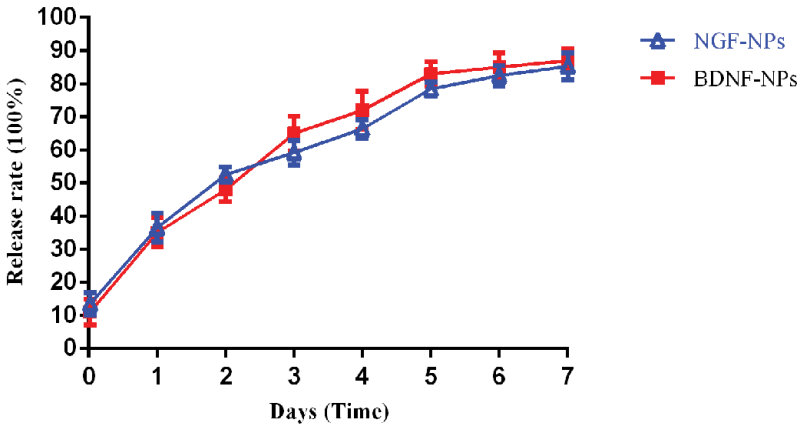

Figure 2: The release rate of BDNF/NGF loading on PEG-PLA nanoparticles over time *in vitro*.

Table 2: Amount-Time profiles of radioactivity in these samples.

Tissue	Amount of DiR loaded PEG-PLA in tissue (cpm/g tissue/g dose × 100 %)					
	5 min (n=3)	30 min (n=3)	2 h (n=3)	6 h (n=3)	12 h (n=3)	24 h (n=3)
Trigeminal nerve	123.91± 65.07	151.24 ± 79.52	9.93 ± 4.70	4.17 ± 1.77	1.06 ± 0.64	0.09 ± 0.01
Olfactory bulb	5.20 ± 1.42	12.53 ± 7.21	1.19 ± 0.31	0.09 ± 0.01	0.006 ± 0.001	0.00 ± 0.00
Brain stem	1.28 ± 0.94	4.52 ± 1.35	1.58 ± 0.72	1.01 ± 0.06	0.29 ± 0.02	0.06 ± 0.002

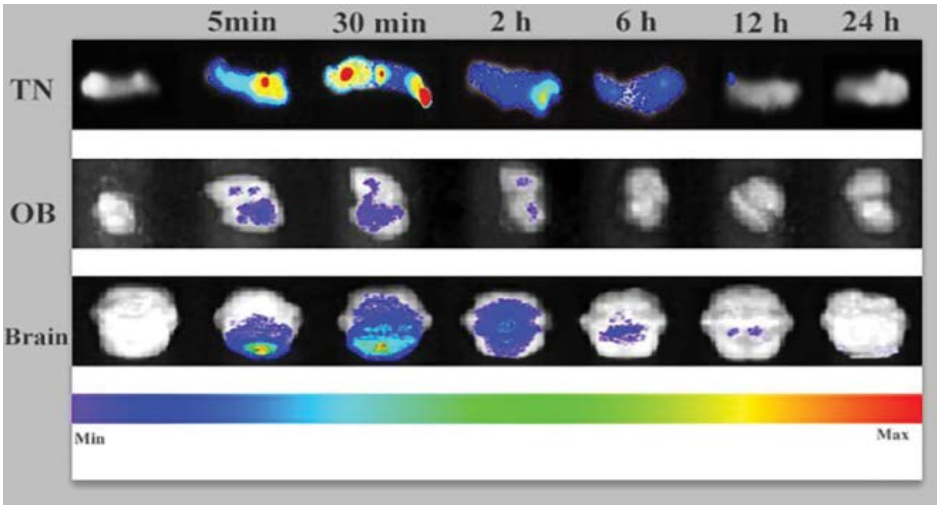

Figure 3: CRi Mastreo small animals imaging system exhibited fluorescence images of trigeminal nerve, olfactory bulb (OB) and brain at 5 min, 30 min, 2 h, 6 h, 12 h and 24 h after intranasal administration of BDNF/NGF loading on PEG-PLA nanoparticles under. The results indicated that most of the nanoparticles were transported to the brain via trigeminal nerve pathway.

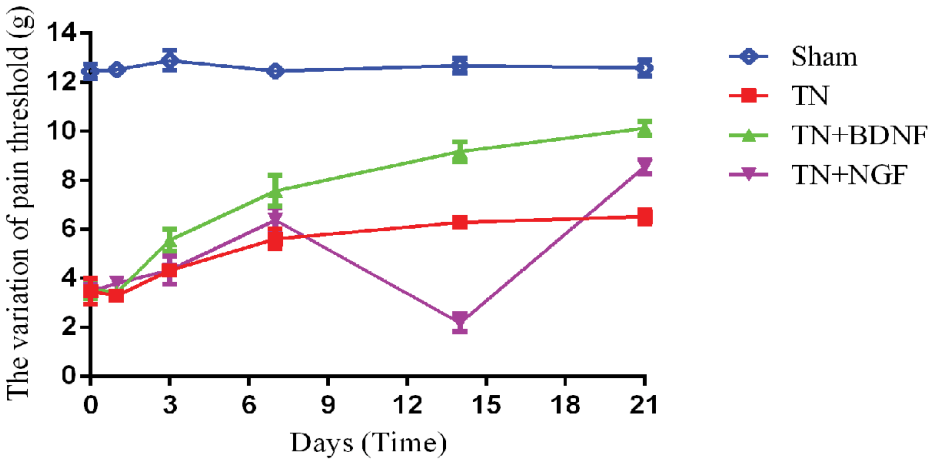

Figure 4: Observation of pain threshold during time in those four groups.

trigeminal nerve in these groups with western blotting. As illustrated in the experiment (**Figure 6**), the results indicated that the level of Nav1.8 and Bax were significantly increased in *group TN* compared with other groups ($p<0.05$). But the level of Bcl-2 and NF-κB were significantly increased in *group TN+BDNF or TN+NGF* compared with *group TN* ($p<0.05$).

RT-PCR

The expression of mRNAs for trigeminal nerve genes of Nav1.8, NF-κB, Bax, Bcl-2 and GAPDH (internal control) was determined by real-time PCR analysis. As illustrated in the

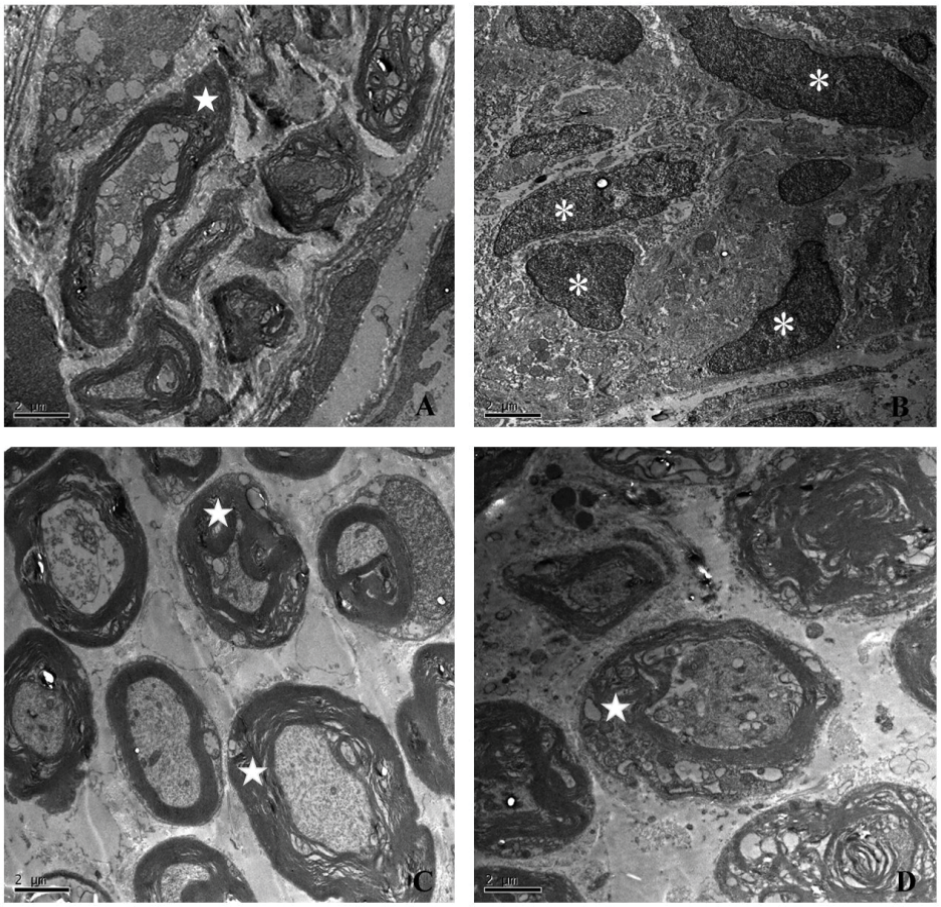

Figure 5: The myelin ultrastructure of trigeminal nerve in these four groups under electron microscopy. Axons ensheathed by schwann cell cytoplasm without the formation of myelin were indicated with an asterisk (*), the noramal axons ensheathed were showed with an pentagram (☆). Demyelination was observed in the *group TN* (B). Low magnification electron micrographs showed the intact myelins with homogeneous density of axon from *group sham* (A), *group TN+BDNF* (C) and g*roup TN+NGF* (D). *Scale bar = 2 μm.* (×5000).

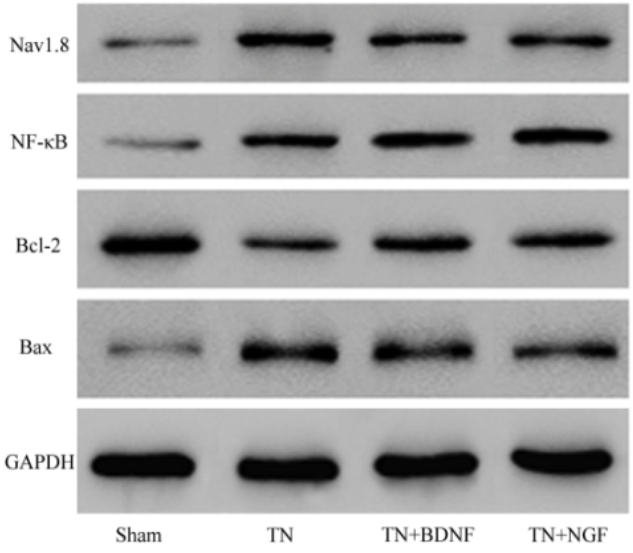

Figure 6: A representative western blot in histoneurology experiment showed that the Nav1.8 and Bax were up-regulated in *group TN*, while the Bcl-2 and NF-κB were up-regulated in *group TN+BDNF* and *group TN+NGF*.

experiment (Figure 7), the results indicated that the level of $Na_v1.8$ and Bax were significantly increased in *group TN* than other groups ($p<0.05$). But the level of Bcl-2 and NF-κB were significantly increased in *group TN+BDNF* and *TN+NGF* than *group TN* ($p<0.05$).

Cell culture

We also investigated the effects of NGF-NPs and BDNF-NPs on the expression of schwann cells. After 6-hour incubation, the amount of schawann cells in *group TN+BDNF* and *TN+NGF* were much than group TN but less than *group sham* (Figure 8).

CCK8 assay

The cell growth and viability were measured using cell proliferation reagent WST-8. The

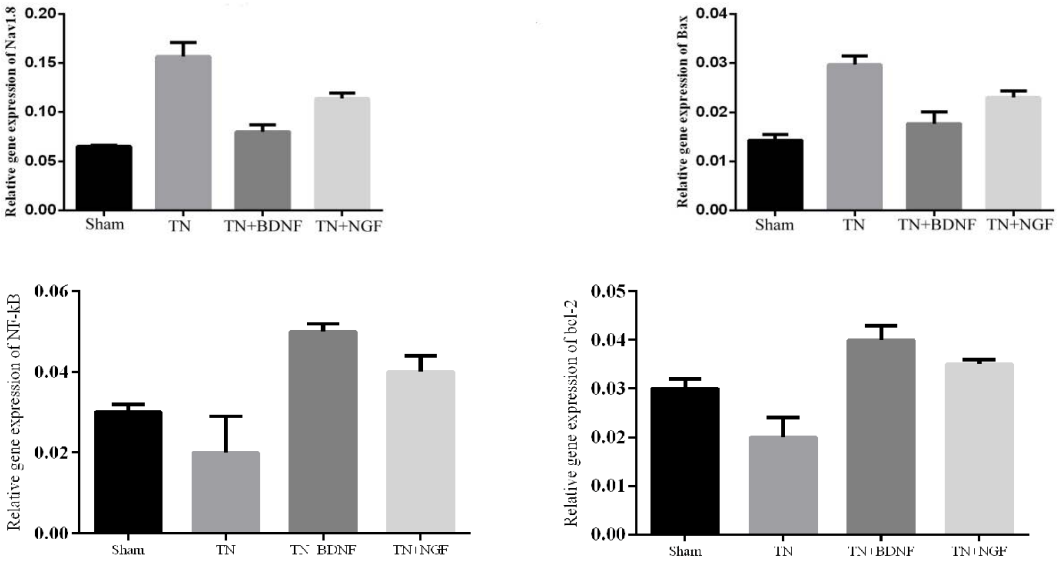

Figure 7: RT-PCR in histoneurology experiment indicated that the level of $Na_v1.8$ and Bax were significantly increased in *group TN* than other groups ($p<0.05$). But the level of Bcl-2 and NF-κB were significantly increased in *group TN+BDNF* and *TN+NGF* than *group TN* ($p<0.05$).

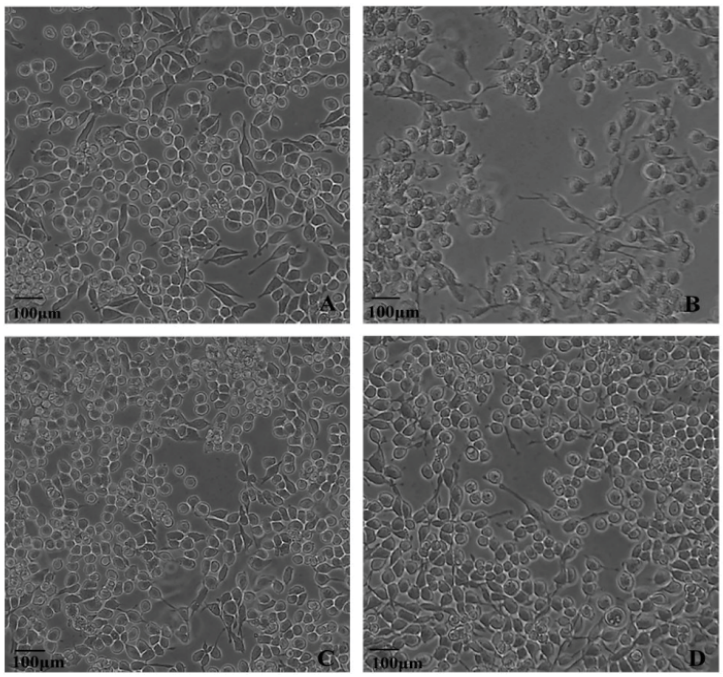

Figure 8: Electron microscopy exhibited the schwann cell in these four groups. *Scale bar = 20μm. A: group sham; B: group TN; C: group TN+BDNF; D: group TN+NGF.* (×100).

cell vitality in *group sham, TN ,TN+BDNF and TN+NGF* was 63%, 33%, 48% and 44%, respectively **(Figure 9)**.

■ Immunostaining

We used the expression of S-100 to estimate the Schwann cells of four groups. The expression of the S-100 protein was demonstrated in the cytoplasm of the cells **(Figure 10)** (×200). The positive rate of *group TN+BDNF* and *TN+NGF* was obviously high than *group TN*, but low than *group sham* **(Figure 11)** ($p<0.05$).

Discussion

As one of the neurotrophic factor, BDNF or NGF may encourage the growth of axon and differentiation of new neurons and synapses [19,20]. Intranasal delivery of BDNF or NGF provides a non-invasive method of bypassing the

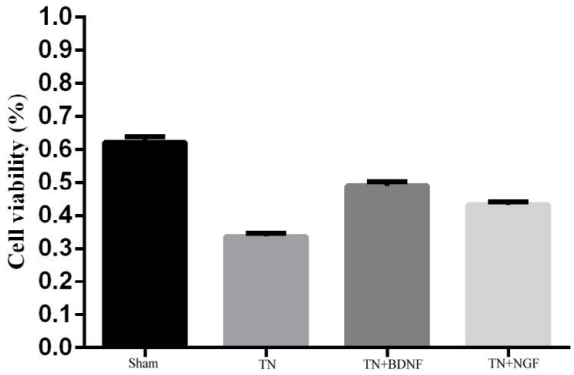

Figure 9: The schwann cell viabilities in these four groups.

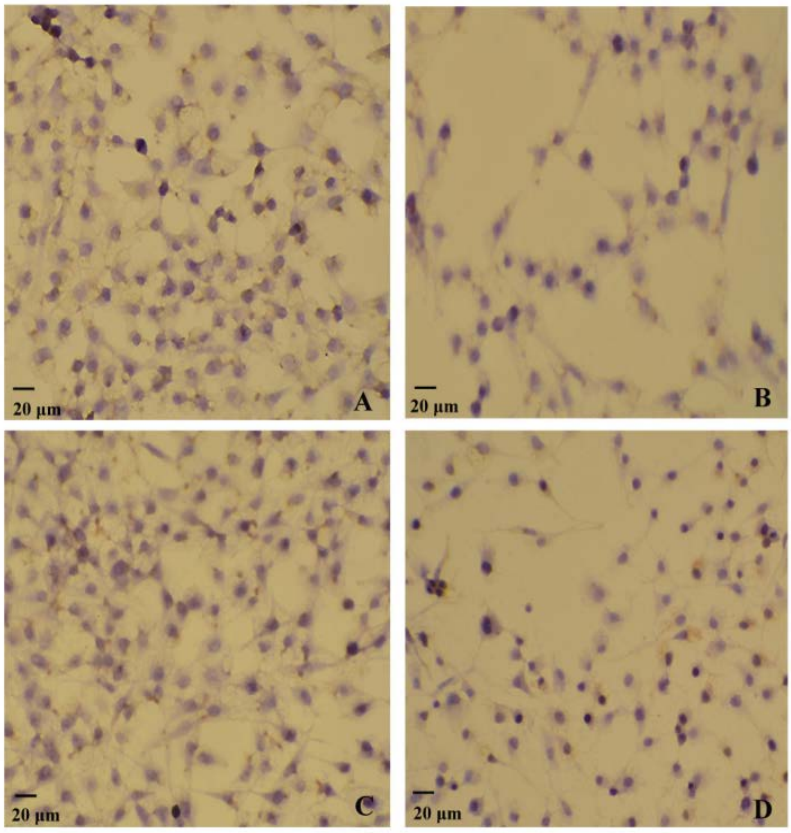

Figure 10: Immunocytochemistry of S-100 in these four groups. *A: group sham; B: group TN; C: group TN+BDNF; D: group TN+NGF*. Schwann cells were used as a positive control. *Scale bar = 20 μm.* (×200).

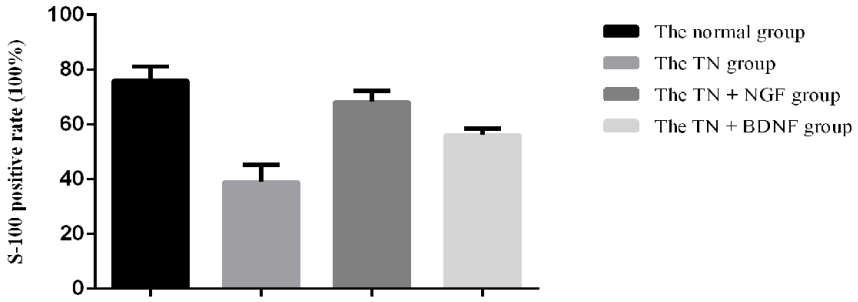

Figure 11: The S-100 positive rate in these four groups.

blood-brain barrier to rapidly deliver therapeutic agents to the brain. The incorporation of the therapeutics mentioned above into nanoparticles might be a promising approach, since colloidal formulations have been shown to protect them the degrading milieu in the nasal cavity and facilitate their transport across the mucosal barriers [17].

In this study, high concentrated nanoparticles were detected by the near infrared fluorescence probe image in the trigeminal nerve. It indicated that the predominant mode of transport into the CNS via the trigeminal nerve pathway. The trigeminal nerve enters the brainstem at the pons and some of its nerve endings terminate beneath the nasal epithelial surface, and the area of the nasal epithelial surface is so huge, this is maybe the reason why the high concentrations of nanoparticles were detected in the intracranial trigeminal nerve [11]. The formation of peripheral myelin is a complex, dynamic process, the schwann cell provide a powerful tool to dissect the complex interaction necessary for the formation of the peripheral myelin by permitting the characterization of three major stages in the process, proliferation, premyelination, and myelination stages [21-23]. When high concentration of NGF-NPs or BDNF-NPs reach the trigeminal nerve, BDNF binds to their neurotrophin receptor of $p75^{NTR}$ and trkB, NGF binds to trkA, which play an important role in schwann cell myelination or the maintenance of myelination of largest regenerating axons [15]. The result of *group TN+NGF* also indicated that NGF is a prominent hyperalgesic meditor in the trigeminal system which seemed to be mediated by activation of TrkA receptors and to involve TRPV1 receptors and mast cells [24].

Previous studies have found the up-regulation of Nav1.8 in trigeminal nerve [25-27]. As the trigeminal root is compressed, the nerve fibers are demyelinated, which induces the Nav1.8 emerge in the compressed site and leads to subthreshold membrane potential oscillation (SMPO); when the membrane potential reaches the threshold, ectopic action potentials are ignited; when these messy impulses transmit to the central, paroxysmal pain attacks [28]. The western-blotting and RT-PCR also confirmed that the up-regulation of $Na_v1.8$ after the infraorbital nerve was constricted, but after the treatment of BDNF-NPs or NGF-NPs, the $Na_v1.8$ began to decrease in *group TN + BDNF* and *group TN + NGF*. NF-κB is released from $I_\kappa B_\alpha$, and it is then translocated to the nucleus where it promotes the transcription of a large number of proteins involved in inflammation, apoptosis, and cell proliferation [29]. The apoptosis pathway is regulated by members of the Bcl-2 protein family, which regulate the changes in the permeability of the mitochondrial outer membrane [29]. Bax, a member of the Bcl-2 protein family, initiates apoptosis when it binds to the mitochondrial outer membrane, thereby changing its permeability and releasing apoptotic proteins [29]. The findings in our study demonstrated that BDNF decreased the expression of $Na_v1.8$, Bax and increased the expression of Bcl-2 and NF-κB, which also means that the BDNF has the function of anti-apoptosis.

Conclusions

In the present study, we confirmed that PEG-PLA nanoparticles were effective in mediating BDNF or NGF transport into the brain following intranasal administration via trigeminal nerve pathway. The results indicated that the BDNF-NPs or NGF-NPs could promote the repair of axon growth and prevent the apoptosis. The technique described here could offer an invasive remedy treatment of trigeminal neuralgia.

Funding

This work was supported by the China's government under grant of National Natural Science Foundation (#81471317).

References

1. Unal TC, Unal OF, Barlas O, *et al.* Factors determining the outcome in trigeminal neuralgia treated with percutaneous balloon compression. *World. Neurosurg* 107(1), 69-74 (2017).
2. Gonzalez-Quarante LH, Ruiz-Juretschke F, Agarwal V, *et al.* Microvascular decompression for trigeminal neuralgia using a novel fenestrated clip and tentorial flap technique. *World. Neurosurg* 106(1), 775-784 (2017).
3. Alshukry A, Salburgo F, Jaloux L, *et al.* Trigeminal neuralgia (TN): A descriptive literature analysis on the diagnosis and management modalities. *J. Stomatol. Oral. Maxillofac. Surg* 118(4), 251-254(2017).
4. Xia L, Zhong J, Zhu J, *et al.* Effectiveness and safety of microvascular decompression surgery for treatment of trigeminal neuralgia: a systematic review. *J. Craniofac. Surg* 25(1), 1413-1417(2014).
5. Liu MX, Zhong J, Dou NN, *et al.* Management of symptomatic hemifacial spasm or trigeminal neuralgia, *Neurosurgical. Rev* 39(1), 411-418(2016).
6. Cheng J, Meng J, Liu W, *et al.* Nerve atrophy in trigeminal neuralgia due to neurovascular compression and its association with surgical outcomes after microvascular decompression. *Acta. Neurochir* 159(9), 1699–1705(2017).
7. Cohen J, Mousavi SH, Faraji AH, *et al.* Stereotactic Radiosurgery as Initial Surgical Management for Elderly Patients with Trigeminal Neuralgia. *Stereotact. Funct. Neurosurg* 95(1), 158-165(2017).
8. Zhu J, Zhong J, Jiao W, *et al.* Via-cerebellar-fissures approach for microvascular decompression of trigeminal nerve. *J. Craniofac. Surg* 25(1), 1438-1440(2014).
9. Gubian A, Rosahl SK . Meta-Analysis on Safety and Efficacy of Microsurgical and Radiosurgical Treatment of Trigeminal Neuralgia. *World. Neurosurg* 103(1), 757-767(2017).
10. Roberts VL, Fews D, McNamara JM, *et al.* Trigeminal Nerve Root Demyelination Not Seen in Six Horses Diagnosed with Trigeminal-Mediated Headshaking. *Frontiers. Vet. Sci* 4(1), 72(2017).
11. Xia L, Liu MX, Zhong J, *et al.* Fatal complications following microvascular decompression: could it be avoided and salvaged?, Neurosurgical review 40(1), 389-396(2017).
12. Zhong J. An ideal microvascular decompression technique should be simple and safe. *Neurosurg. Rev* 35(1), 137-140(2012).
13. Zhong J, Li ST, Zhu J, *et al.* A clinical analysis on microvascular decompression surgery in a series of 3000 cases. *Clin. Neurol. Neurosurg* 114(1), 846-51(2012).
14. Chan JR, Cosgaya JM, Wu YJ, *et al.* Neurotrophins are key mediators of the myelination program in the peripheral nervous system. *Proc. Natl. Acad. Sci* 98(1), 14661-14668(2001).
15. Takeda M, Takahashi M, Kitagawa J, *et al.* Brain-derived neurotrophic factor enhances the excitability of small-diameter trigeminal ganglion neurons projecting to the trigeminal nucleus interpolaris/caudalis transition zone following masseter muscle inflammation. *Mol. Pain* 9(1), 49(2013).
16. Gao X, Wu B, Zhang Q, *et al.* Brain delivery of vasoactive intestinal peptide enhanced with the nanoparticles conjugated with wheat germ agglutinin following intranasal administration.↑ *J. Control. Release* 121(1), 156-67(2007).
17. Liu Q, Shen Y, Chen J, *et al.* Nose-to-brain transport pathways of wheat germ agglutinin conjugated PEG-PLA nanoparticles. *Pharm. Res* 29(1): 546-58(2012).
18. Stern E, Forsythe AB, Youkeles L, *et al.* A cytological scale for cervical carcinogenesis. *Cancer Res* 34 2358-2361(1974).
19. Kimura A, Namekata K, Guo X, *et al.* Neuroprotection, Growth Factors and BDNF-TrkB Signalling in Retinal Degeneration. *Int. J. Mol. Sci* 17(2016).
20. Price TJ, Louria MD, Candelario-Soto D, *et al.* Treatment of trigeminal ganglion neurons in vitro with NGF, GDNF or BDNF: effects on neuronal survival, neurochemical properties and TRPV1-mediated neuropeptide secretion. *BMC. Neurosci* 6(1), 4(2005).
21. Li R, Zou S, Wu Y, *et al.* Heparin-based coacervate of bFGF facilitates peripheral nerve regeneration by inhibiting endoplasmic reticulum stress following sciatic nerve injury. *Oncotarget* 8(1), 48086-48097(2017).
22. Sakai K, Shimba K, Kotani K, *et al.* A co-culture microtunnel technique demonstrating a significant contribution of unmyelinated Schwann cells to the acceleration of axonal conduction in Schwann cell-regulated peripheral nerve development. *Integr. Biol* 678-686(2017).
23. Sowa Y, Kishida T, Tomita K, *et al.* Direct Conversion of Human Fibroblasts into Schwann Cells that Facilitate Regeneration of Injured Peripheral Nerve In Vivo. *Stem. Cells. Transl. Med* 6(1), 1207-1216(2017).
24. Dos Reis RC, Kopruszinski CM, Nones CF, et al. Nerve growth factor induces facial heat hyperalgesia and plays a role in trigeminal neuropathic pain in rats. *Behav. Pharmacol* 27(1): 528-535(2016).
25. Liang J, Liu X, Pan M, et al. Blockade of Nav1.8 currents in nociceptive trigeminal neurons contributes to anti-trigeminovascular nociceptive effect of amitriptyline. Neuromolecular medicine 16(1), 308-321(2014).
26. Bird EV, Christmas CR, Loescher AR, *et al.* Correlation of Nav1.8 and Nav1.9 sodium channel expression with neuropathic pain in human subjects with lingual nerve neuromas. *Mol. Pain* 9(1), 52(2013).
27. Stirling LC, Forlani G, Baker MD, *et al.* Nociceptor-specific gene deletion using heterozygous NaV1.8-Cre recombinase mice. *Pain* 113(1), 27-36(2005).
28. Choi JS, Waxman SG. Physiological interactions between Na(v)1.7 and Na(v)1.8 sodium channels: a computer simulation study. *J. Neurophysiol* 106(1), 3173-3184(2011).
29. Kim CS, Choi JS, Joo SY, *et al.* Nicotine-Induced Apoptosis in Human Renal Proximal Tubular Epithelial Cells. *PLoS .One* 11(1), e0152591(2016).